

Space-Time Coding Schemes for MDL-Impaired Mode-Multiplexed Fiber Transmission Systems

Elie Awwad, Ghaya Rekaya-Ben Othman, and Yves Jaouën

Abstract—Spatial division multiplexing (SDM) holds out the prospects of increasing the capacities of optical fiber transmission links, especially with the recent achievements in the design of few-mode fibers and few-mode optical amplifiers. However, these systems are impaired by the capacity-limiting mode dependent loss (MDL) arising from imperfections in the optical fiber and inline components. Optical solutions were suggested to reduce, yet not completely remove, the accumulated MDL in the link through the use of strong coupling fibers and mode scramblers. Inspired by our previous study on mitigating polarization dependent loss (PDL), we present space-time (ST) coding schemes to mitigate MDL in mode-multiplexed optical transmission systems. We show, for the first time, that the combination of redundancy-free ST coding solutions with inline mode scrambling and optimal maximum-likelihood (ML) detection can completely absorb the SNR penalties induced by the MDL. The performance was assessed through simulations of three- and six-mode multiplexed systems where MDL levels up to 10 dB were observed. However, given the increased computational complexity of the suggested ML-decoded ST schemes, we present two reduced-complexity ST solutions offering a near-optimal performance. The first one consists in using a sub-optimal decoder and the second is a multiblock ST coding approach that can be scaled up for larger SDM systems.

Index Terms—Fiber optics communications, MIMO, space division multiplexing, space-time coding.

I. INTRODUCTION

OPTICAL fiber communication systems have known important and steady evolution for the last decades in order to meet the increasing demand for higher capacities in today's information-driven environments. The ever-growing number of users and machines connected to the Internet urged the need to increase the data carrying capacity of every single optical fiber in the backbone of the global telecommunication system. This evolution involved the exploration and optimal use of the following degrees of freedom of standard single mode fibers in currently deployed systems: time, wavelength, phase and polarization. To keep up with the rising demands, an additional degree of freedom, *space* is being widely investigated today to achieve the next leap in capacity [1]–[4]. Spatial division multiplexing (SDM) had been experimentally demonstrated through different approaches including multi-core fiber (MCF) solutions where several coupled or uncoupled cores coexist in the same

cladding, or multi-mode fiber (MMF) solutions where the fiber core is enlarged to allow the propagation of several linearly polarized (LP) modes, or even a combination of both (MCF where each core is multi-mode) [1], [5]–[7]. The main advantage of these SDM techniques is the provision of an orthogonal set of pathways that can carry independent data streams in the same fiber while answering integration constraints of system components, i.e., components that operate on all the modes such as mode couplers [8], optical amplifiers [9], [10], and wavelength selective switches (WSSs) [11], thus aiming to reduce the cost per bit and energy consumption of the system.

However, while offering interesting multiplexing capabilities, SDM adds a primary challenge which is the management of crosstalk caused by the packing of several channels in the same fiber. In MCFs, the crosstalk increases when reducing the inter-core distances while in MMFs, LP modes overlap significantly in the single core, and the carried data streams couple randomly during the propagation. LP modes will also endure differential losses or gains leading to modal loss disparities. In this paper, we will focus on the management of the loss disparities in mode division multiplexed (MDM) optical transmission systems. This focus is driven, on one hand, by the emergence of new fabrication processes of few-mode optical components such as few-mode fibers (FMFs) [7] and few-mode amplifiers (FMAs) that are gaining in maturity.

Another substantive reason for the current interest in MDM systems is the integration of coherent detection and digital signal processing (DSP) techniques to electronically manage modal crosstalk at the receiver using multiple-input-multiple-output (MIMO) filters. Originally developed for wireless systems, MIMO signal processing has been successfully applied to undo channel crosstalk and retrieve the transmitted data by processing all the received data streams at the same time (from antennas in multi-antenna wireless channels, from polarization states in Pol-Mux systems [12], [13] or from modes in MDM systems). If the data streams remain orthogonal and their total energy is conserved after propagating through the transmission system, the channel would be equivalent to a unitary transformation, and hence a channel inversion would be enough in order to separate the streams and retrieve the performance of a crosstalk-free additive white Gaussian noise (AWGN) channel. However, long-haul MDM systems are impaired by modal loss disparities, also known as mode dependent loss (MDL), arising from imperfections in the link such as non-unitary couplings in the fiber due to bending losses and splices [14] as well as MDLs/gains in optical components such as FMAs and WSSs [9]–[11]. MDL deteriorates the overall system performance [14], [15] because the data-carrying streams interweave

Manuscript received June 2, 2015; revised September 18, 2015; accepted October 19, 2015. Date of publication October 26, 2015; date of current version November 18, 2015.

The authors are with the Department of Communication and Electronics, TELECOM ParisTech, Paris 75634, France (e-mail: elie.awwad@telecom-paristech.org).

Color versions of one or more of the figures in this paper are available online at <http://ieeexplore.ieee.org>.

Digital Object Identifier 10.1109/JLT.2015.2495343

while experiencing different levels of attenuation and lose their orthogonality [2], [16]. Hence, MDL is definitely a challenge that needs to be surmounted.

In order to reduce MDL arising from in-line components in long-haul optical links, fibers with strongly coupled modes [15] and mode scramblers [14], [17] were suggested to average the losses experienced by each mode, thus reducing the accumulated MDL. While these optical solutions reduce MDL, they are not able to completely eliminate it. Moreover, some stringent requirements are needed in order to obtain the desired MDL reduction (fiber design, number of mode scramblers in the link...). On the other hand, in [15], Lobato *et al.* used an optimal maximum-likelihood (ML) detection instead of a zero-forcing (ZF) equalizer to enhance the performance of MDL-impaired MDM systems. This is expected for sure in presence of MDL due to the enhancement of noise by the channel inversion operation of the ZF equalizer that leads to a sub-optimal detection. In [18], the same authors proposed two alternatives to the high-complexity exhaustive search ML detection: a reduced-complexity sub-optimal version and the well-known sphere decoder (SD) [19]. However, we will show that more gains can be obtained with MIMO coding techniques.

In this work, we propose space-time (ST) coding, originally designed to combat multipath fading in wireless MIMO systems, as a DSP solution to mitigate MDL in the optical channel. Applying ST codes to polarization-multiplexed systems showed their efficiency in mitigating polarization dependent loss (PDL) [20] and provided an insight into considering them for MDM systems. In [21], we showed the efficiency of ST coding in mitigating MDL generated by fiber imperfections in three-mode MDM systems. In [22], Okonkwo *et al.* also suggested a ST architecture to enhance the performance of a three-mode system by repeating a delayed version of the same data symbol over the different modes. While this architecture offers OSNR gains, it inherently reduces the multiplexing gain of the MDM system. In this paper, we show that redundancy-free ST schemes can be applied to mitigate MDL and enhance system performance while maintaining the multiplexing gains. The performance of three- and six-mode MDM schemes is investigated where FMAs, one of the major sources of MDL, are considered: first, we define a channel model and study the MDL-induced penalties in a single-polarization MDM scheme. A single-polarization hypothesis is considered to solely focus on loss disparities between spatial modes. Second, we apply ST codes at the transmitter along with optimal ML detection at the receiver to mitigate MDL. We show, for the first time, a complete mitigation of MDL levels as high as 10 dB in a six-mode MDM Orthogonal frequency division multiplexing (OFDM) system. Later, we analyze the complexity of the proposed ST coding solution to evaluate the scale-up possibilities to larger MDM systems. Consequently, we suggest two low-complexity scalable schemes that maintain the MDL-induced penalty low. The first uses a sub-optimal detection, the ZF with decision feedback equalization (ZF-DFE) and the second scheme consists of a new multi-block coding approach.

II. MDM OPTICAL TRANSMISSION SYSTEMS

A. System Model

Long-haul MDM systems give rise to linear impairments that must be mitigated in order to retrieve the transmitted data. We focus in this section on the most challenging impairments that include differential modal group dispersion (DMGD) in FMFs, modal crosstalk as well as MDL. Then, based on models suggested in previous works [14], [15], [23], we define and simulate a channel model of an MDL-impaired mode-multiplexed transmission.

1) *Differential Modal Group Dispersion*: In FMFs, DMGD between different modes results in temporal inter-symbol interference. Moreover, these modes spatially mix during propagation which requires MIMO equalization techniques to retrieve the multiplexed signals at the receiver side. Given M propagating modes, the equalizing filter consists of $M \times M$ matrices that will completely compensate unitary crosstalk and dispersion provided that the filter is larger than the maximum delay spread between modes [24]. Computational complexities of several time-domain and frequency-domain equalizers (FDE) in both single-carrier (SC) and multi-carrier formats were studied [25]. OFDM and SC-FDE were found to achieve the lowest complexities for long-haul MDM systems with a small advantage for OFDM [25].

2) *Crosstalk & Fiber Model*: The propagating modes spatially overlap in the fiber due to imperfections in doping and asymmetries caused by mechanical or thermal stress and micro-bends. Hence, the symbols carried by each mode couple randomly along the fiber. This coupling can be unitary and lossless as modeled in [26], [27] or non-unitary and lossy as modeled in [23] depending on the fiber designs and the sources of imperfections. Two coupling strategies were recently investigated: low crosstalk levels [28], [29] to avoid the use of complex MIMO processing at the receiver, or strong coupling with a full MIMO processing [24]. Strong coupling can be positively exploited to reduce both the DMGD spread and the accumulated MDL because both effects follow a random-walk process in presence of strong coupling, and thus scale with the square-root of the fiber length or the number of MDL sources in the link, rather than scaling linearly [16], [30].

In our model, we intentionally choose to keep the fiber-generated coupling unitary, neglecting any distributed MDL at imperfect splices and micro-bends, to solely focus on the accumulated MDL generated by discrete inline components. Recent works showed the possibility of realizing low-splice losses of FMF sections [31] and some initial transmission experiments over 30 km [7] to 96 km [24] of FMFs have also shown a negligible fiber-generated MDL. We model each fiber span as a concatenation of K independent sections:

$$\mathbf{F}_{\text{span}, M \times M} = \prod_{k=1}^K (\mathbf{T}_k \mathbf{R}_k) \quad (1)$$

Each section is a product of a diagonal matrix \mathbf{T}_k with random phase entries and a real orthogonal rotation matrix \mathbf{R}_k

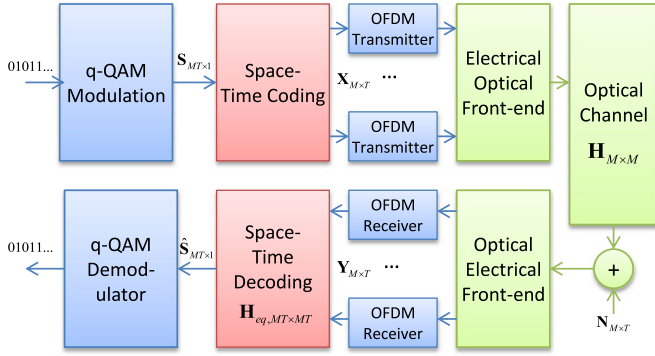


Fig. 1. ST coded MDM OFDM transmission system.

representing the distributed modal crosstalk. In order to generate these rotation matrices for any number of modes, the mode coupling angles of \mathbf{R}_k will be computed using the crosstalk levels generated at displaced cores of two fiber sections. These crosstalk levels are computed by an overlap integral of the electrical field distributions of the propagating modes over the fiber cross section as in [14]:

$$c_{M1-M2} = \iint_A E_{M1}(x, y) E_{M2}^*(x + \Delta x, y + \Delta y) dA \quad (2)$$

where $M1$ and $M2 \neq M1$ are two different guided modes, A is the fiber cross section, E is the normalized complex field, Δx and Δy are the misalignment values. It is important to mention that overlap integrals at a core misalignment are used to emulate modal coupling. In case a real misalignment was present, the resulting crosstalk matrix would not be unitary [14]. This emulation technique was motivated by an observation in [32] where authors noted that crosstalk levels computed from overlap integrals were equal to the ones computed from the coupled-mode theory. $M(M-1)/2$ crosstalk values are needed corresponding to the number of Euler angles in the rotation matrix. The misalignments Δx and Δy for each section are drawn from a uniform distribution over $[-\sigma r_c : \sigma r_c]$ where σ is a percentage of the core radius r_c that sets the coupling strength.

3) *Mode Dependent Loss*: In long-haul MDM systems, MDL arises mainly from imperfect inline components such as optical amplifiers and WSSs [14], [15], [33], [34]. Unlike dispersion, MDL reduces the capacity of the MIMO channel because the data-carrying spatial modes interweave while observing various attenuation levels which breaks the orthogonality of these modes and result in a loss of information that is irreversible at the receiver side. Hence, it is crucial to maintain low MDL levels in the link. Due to technological limits (the need of tailored doping profiles, specific spatial distribution of pumping power in FMAs), it is quite hard to maintain gain offsets in the optical components lower than 2 dB for more than 6 spatial modes, especially for FMAs [9], [10].

4) *Complete Channel Model*: We define an MDM OFDM transmission system, as shown in Fig. 1, with 3 (resp. 6) propagating modes: the fundamental mode LP_{01} and the two degeneracies LP_{11a} and LP_{11b} of the LP_{11} mode (resp. these three modes, the LP_{02} as well as the degeneracies LP_{21a} and LP_{21b}

of the LP_{21} mode). Though unrealistic, we consider a single polarization per spatial mode in order to concentrate only on differential modal losses as done in several studies on MDL [14], [16], [23]. We neglect any fiber non-linearity and focus on the linear impairments of the system. An OFDM signal with a suitable cyclic prefix modulates each spatial mode. The long-haul optical link contains FMFs and amplifiers with modal gain offsets. In absence of laser phase noise and frequency offsets, the resulting MIMO channel per OFDM subcarrier is given by:

$$\begin{aligned} \mathbf{Y}_{M \times T} &= \mathbf{H}_{M \times M} \mathbf{X}_{M \times T} + \mathbf{N}_{M \times T} \\ &= \sqrt{\alpha} \prod_{l=1}^L (\mathbf{P}_l \mathbf{G}_l \mathbf{F}_l) \mathbf{X}_{M \times T} + \mathbf{N}_{M \times T} \end{aligned} \quad (3)$$

where $\mathbf{X}_{M \times T}$ (resp. $\mathbf{Y}_{M \times T}$) are the emitted (resp. the received) complex symbols on the $M = \{3, 6\}$ modes and during T time slots. $\mathbf{H}_{M \times M}$ is the linear channel matrix consisting of L independent fiber spans \mathbf{F}_l given by (1), followed each by an FMA modeled as a diagonal matrix \mathbf{G}_l , as well as a mode scrambler \mathbf{P}_l . The gains in \mathbf{G}_l are assigned as follows: the LP_{01} mode has a unit gain and gain offsets $\Delta G_{01-\mu\nu}$ are defined for each $LP_{\mu\nu}$ mode. \mathbf{P}_l are random permutation matrices representing perfect mode mixers as in [14]. α is a normalization factor compensating common losses. In a real system, MDL can be frequency-dependent with a coherence bandwidth dictated by the amount of modal dispersion in the link [16], [33]. In [35], the frequency averaged MDL estimated from a 10×50 km six-mode WDM-SDM experiment was relatively wavelength-independent across the C-band. As a first approach, modal dispersion has not been considered, as done in recent studies [14], [36], to limit the current investigation to a single wavelength or to a frequency-flat channel. Finally, $\mathbf{N}_{M \times T}$ is an additive noise assumed to be zero-mean white Gaussian of variance $2N_0$ per complex dimension per mode added at the receiver. In a long-haul optical link, the dominant noise is amplified spontaneous emission generated at each amplification stage. Hence, it is subject to MDL and can become spatially colored. In [16], Ho *et al.* showed that with strong modal coupling, the spatial non-whiteness of the noise can be neglected when the number of noise sources in the link increases. In our model, the hypothesis of a white noise will be maintained for all coupling levels as it was done in recent works [14], [18], [36], and the study of noise correlation will be left for a future study.

Before introducing ST codes, we look into the statistics of MDL in the defined channel model under different coupling scenarios. We consider an MDM system with $L = 8$ spans where FMFs have a parabolic index profile with a core radius of $8.7 \mu\text{m}$ and a numerical aperture of 0.205 at $\lambda = 1550$ nm, thus supporting 6 modes. Each span consists of $K = 200$ sections. The amplifiers present the following gain offsets $\Delta G_{01-11} = -1.3$ dB, $\Delta G_{01-21} = -2$ dB and $\Delta G_{01-02} = -0.2$ dB corresponding to a promising FMA design with optimized gain offsets presented in [10], and are followed by a mode scrambler. For $K = 200$ sections, three coupling strengths are investigated by drawing misalignments from a uniform distribution with σ tuned to 0.6%, 3% and 5% of the core radius r_c to emulate weak, medium and strong modal coupling respectively. 10^6 channel

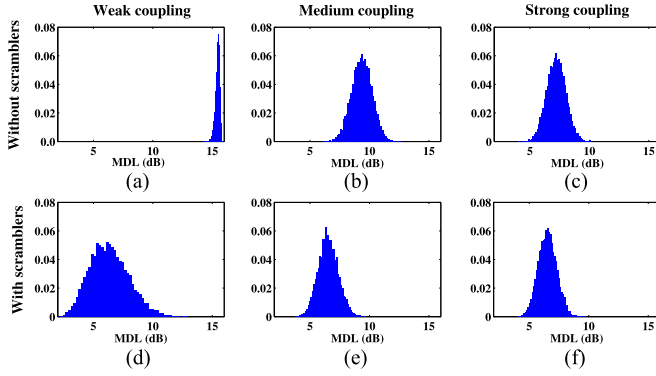


Fig. 2. Simulated probability distribution functions of MDL in the investigated 6×6 MDM system in different coupling and scrambling scenarios (8 spans, 2 dB of MDL per span).

realizations were numerically simulated and the corresponding MDL levels were computed for each scenario, MDL being defined as the ratio in dB between the squares of the highest and the lowest singular values of \mathbf{H} . The obtained MDL distributions are shown in Fig. 2. First, we notice that coupling and scrambling significantly reduce the average MDL as well as its variance. With weak-coupling fiber spans, the 2 dB MDL of each amplifier sums up resulting in an accumulated MDL of $8 \times 2 = 16$ dB. At medium coupling, the modes are only partially correlated and the average MDL decreases to 10 dB. Strong coupling and mode scrambling reduces the average MDL to 6 dB which is close to $\sqrt{8} \times 2 = 5.7$ dB, the expected accumulated MDL value when full, random coupling occurs between

identical MDL sources [16]. Hence, strong coupling in FMFs is desirable in order to reduce the accumulated MDL as it does with the DMGD spread [16]. However, in all cases, MDL cannot be eliminated completely.

B. ST Coding

Conventional optical MIMO schemes use simple data multiplexing which consists, in the MDM case, in sending a vector $\mathbf{S}_{M \times 1}$ of independent symbols (q-quadratic-amplitude modulation (QAM) for instance) on M modes at a single time slot. However, we can make better use of the “space” and “time” dimensions of the MDM MIMO scheme by inserting the same data symbol in newly-formed linear combinations sent over different modes at different time slots. Then, at the receiver, the copies can be exploited to enhance the performance since the same data symbol would have experienced various channel states, hence the loss disparities between the data streams would be further reduced. This technique is known as ST coding and was originally designed for wireless MIMO communications to combat Rayleigh fading [37].

Many ST code families were designed for wireless MIMO schemes. We will focus on a specific category of codes: ST block codes (STBC) in which a codeword is represented by a matrix $\mathbf{X}_{M \times T}$, where T is the number of time slots over which the code is defined. It is obtained by multiplying a symbol vector $\mathbf{S}_{MT \times 1}$ with a generator matrix \mathbf{M}_G and rearranging the obtained vector into an $M \times T$ matrix. This operation takes place at the transmitter side in the “ST Coding” block in Fig. 1.

$$\mathbf{X}_{\mathcal{T}, 3 \times 3} = \frac{1}{\sqrt{3}} \begin{bmatrix} s_1 + \theta s_2 + \theta^2 s_3 & \phi^2(s_4 + j\theta s_5 + j^2\theta^2 s_6) & \phi(s_7 + j^2\theta s_8 + j\theta^2 s_9) \\ \phi(s_7 + \theta s_8 + \theta^2 s_9) & s_1 + j\theta s_2 + j^2\theta^2 s_3 & \phi^2(s_4 + j^2\theta s_5 + j\theta^2 s_6) \\ \phi^2(s_4 + \theta s_5 + \theta^2 s_6) & \phi(s_7 + j\theta s_8 + j^2\theta^2 s_9) & s_1 + j^2\theta s_2 + j\theta^2 s_3 \end{bmatrix} \quad (4)$$

$$\text{vec}_{\mathbb{C}}(\mathbf{X}_{\mathcal{T}, 3 \times 3}) = \mathbf{M}_{G, 9 \times 9} \mathbf{S}_{9 \times 1}$$

$$= \frac{1}{\sqrt{3}} \begin{bmatrix} 1 & \theta & \theta^2 & 0 & 0 & 0 & 0 & 0 & 0 \\ 0 & 0 & 0 & 0 & 0 & 0 & \phi & \phi\theta & \phi\theta^2 \\ 0 & 0 & 0 & \phi^2 & \phi^2\theta & \phi^2\theta^2 & 0 & 0 & 0 \\ 0 & 0 & 0 & \phi^2 & \phi^2j\theta & \phi^2j^2\theta^2 & 0 & 0 & 0 \\ 1 & j\theta & j^2\theta^2 & 0 & 0 & 0 & 0 & 0 & 0 \\ 0 & 0 & 0 & 0 & 0 & 0 & \phi & \phi j\theta & \phi j^2\theta^2 \\ 0 & 0 & 0 & 0 & 0 & 0 & \phi & \phi j^2\theta & \phi j\theta^2 \\ 0 & 0 & 0 & \phi^2 & \phi^2j^2\theta & \phi^2j\theta^2 & 0 & 0 & 0 \\ 1 & j^2\theta & j\theta^2 & 0 & 0 & 0 & 0 & 0 & 0 \end{bmatrix} \begin{bmatrix} s_1 \\ s_2 \\ s_3 \\ s_4 \\ s_5 \\ s_6 \\ s_7 \\ s_8 \\ s_9 \end{bmatrix} \quad (5)$$

$$\mathbf{X}_{\mathcal{T}, 6 \times 6} = \frac{1}{\sqrt{6}} \begin{bmatrix} f_1(\mathbf{s}_1) & \phi^{\frac{5}{6}} f_2(\mathbf{s}_6) & \phi^{\frac{4}{6}} f_3(\mathbf{s}_5) & \phi^{\frac{3}{6}} f_4(\mathbf{s}_4) & \phi^{\frac{2}{6}} f_5(\mathbf{s}_3) & \phi^{\frac{1}{6}} f_6(\mathbf{s}_2) \\ \phi^{\frac{1}{6}} f_1(\mathbf{s}_2) & f_2(\mathbf{s}_1) & \phi^{\frac{5}{6}} f_3(\mathbf{s}_6) & \phi^{\frac{4}{6}} f_4(\mathbf{s}_5) & \phi^{\frac{3}{6}} f_5(\mathbf{s}_4) & \phi^{\frac{2}{6}} f_6(\mathbf{s}_3) \\ \phi^{\frac{2}{6}} f_1(\mathbf{s}_3) & \phi^{\frac{1}{6}} f_2(\mathbf{s}_2) & f_3(\mathbf{s}_1) & \phi^{\frac{5}{6}} f_4(\mathbf{s}_6) & \phi^{\frac{4}{6}} f_5(\mathbf{s}_5) & \phi^{\frac{3}{6}} f_6(\mathbf{s}_4) \\ \phi^{\frac{3}{6}} f_1(\mathbf{s}_4) & \phi^{\frac{2}{6}} f_2(\mathbf{s}_3) & \phi^{\frac{1}{6}} f_3(\mathbf{s}_2) & f_4(\mathbf{s}_1) & \phi^{\frac{5}{6}} f_5(\mathbf{s}_6) & \phi^{\frac{4}{6}} f_6(\mathbf{s}_5) \\ \phi^{\frac{4}{6}} f_1(\mathbf{s}_5) & \phi^{\frac{3}{6}} f_2(\mathbf{s}_4) & \phi^{\frac{2}{6}} f_3(\mathbf{s}_3) & \phi^{\frac{1}{6}} f_4(\mathbf{s}_2) & f_5(\mathbf{s}_1) & \phi^{\frac{5}{6}} f_6(\mathbf{s}_6) \\ \phi^{\frac{5}{6}} f_1(\mathbf{s}_6) & \phi^{\frac{4}{6}} f_2(\mathbf{s}_5) & \phi^{\frac{3}{6}} f_3(\mathbf{s}_4) & \phi^{\frac{2}{6}} f_4(\mathbf{s}_3) & \phi^{\frac{1}{6}} f_5(\mathbf{s}_2) & f_6(\mathbf{s}_1) \end{bmatrix} \quad (6)$$

In this category, we will choose codes for 3×3 and 6×6 MDM channels that fulfill the following requirements: first, the codeword matrices are square ($M = T$) in order to place each data symbol on a different mode at each time slot. Second, full-rate codes will be used meaning that M^2 different q-QAM information symbols are sent in each codeword, which does not reduce the multiplexing gain of the MDM system. Third, a uniform average energy will be transmitted per mode. A code family well-known for its generality and performance that meets these requirements is the linear threaded algebraic space-time codes (TAST) [38].

The 3×3 TAST codeword is given above in (4) shown at the bottom of the previous page, where $\phi = \exp(i\pi/36)$, $j = \exp(i2\pi/3)$, $\theta = \exp(i\pi/9)$ and $s_{k=1:9}$ are q-QAM symbols. ϕ and θ are chosen to maximize the coding and diversity gains over a wireless Rayleigh fading 3×3 multi-antenna channel [38]. 9 q-QAM symbols are sent on three time slots in each codeword, achieving a rate of three symbols/time slot. Another way of representing the code consists in vectorizing, column-wise, (4) into (5), shown at the bottom of the previous page, where \mathbf{M}_G is the generator matrix of the code and is unitary ($\mathbf{M}_G \mathbf{M}_G^\dagger = \mathbf{I}_{9 \times 9}$). Hence, we do not increase the energy of the new transmitted symbols after encoding the q-QAM information symbols. The 6×6 TAST codeword is given in (6), shown at the bottom of the previous page, where $\phi = \exp(i\pi/12)$, $\mathbf{s}_{1..6}$ a vector of six q-QAM symbols, $f_n(\mathbf{x}) = \sum_{k=1:6} x_k (j^{n-1} \theta)^{k-1}$ with $j = \exp(i2\pi/6)$, $\theta = \exp(i\pi/18)$. 36 symbols are sent on 6 time slots in each codeword, achieving a full rate of six symbols/time slot. Its unitary generator matrix can be found in [38].

C. ST Decoding

At the receiver side, the original data symbols are estimated using an ML decoder. Assuming that the channel matrix \mathbf{H} is known (or perfectly estimated) and constant during T time slots, and that all emitted codewords \mathbf{X} are equiprobable, the optimal detection scheme of the channel in (3) should satisfy the ML criterion that consists in estimating the codeword \mathbf{X} with $\hat{\mathbf{X}}_{ML}$ minimizing the following Euclidean distance:

$$\hat{\mathbf{X}}_{ML} = \underset{\mathbf{X}_{M \times T} \in C}{\operatorname{argmin}} \|\mathbf{Y} - \mathbf{H}\mathbf{X}\|^2 \quad (7)$$

where C is the set of all possible transmitted codewords. The ML criterion can be further developed to explicitly show the original q-QAM symbols. To this end, we use a vectorized form of (3) showing the generator matrix of the ST code and define an equivalent channel \mathbf{H}_{eq} [39]:

$$\begin{aligned} \mathbf{Y}'_{MT \times 1} &= \operatorname{vec}_C(\mathbf{Y}) = \begin{bmatrix} \mathbf{H} & \mathbf{0} & \mathbf{0} \\ \mathbf{0} & \ddots & \mathbf{0} \\ \mathbf{0} & \mathbf{0} & \mathbf{H} \end{bmatrix} \operatorname{vec}_C(\mathbf{X}) + \operatorname{vec}_C(\mathbf{N}) \\ &= \mathbf{H}'_{MT \times MT} \mathbf{M}_G \mathbf{S}_{MT \times 1} + \mathbf{N}'_{MT \times 1} \\ &= \mathbf{H}_{\text{eq}} \mathbf{S} + \mathbf{N}' \end{aligned} \quad (8)$$

where \mathbf{M}_G is the generator matrix of the coding scheme. In the case of simple spatial multiplexing without coding, $T = 1$ and \mathbf{M}_G is replaced by the identity matrix. \mathbf{S} is a vector of q-QAM

symbols. Given that \mathbf{H} is a full-rank matrix and \mathbf{M}_G is unitary, the ML decoding rule can be reinterpreted as:

$$\hat{\mathbf{S}}_{ML} = \underset{\mathbf{S}_{MT \times 1} \in C'}{\operatorname{argmin}} \|\mathbf{Y}' - \mathbf{H}_{\text{eq}} \mathbf{S}\|^2 \quad (9)$$

where C' is the set of all possible transmitted q-QAM symbols. The ML criterion can be implemented through an exhaustive search in C' where the norm in (9) has to be computed for all possible combinations of the emitted symbols. In the case of a full-rate square ST code with q-QAM symbols, this leads to q^{M^2} norm computations. Fortunately, lower-complexity decoders satisfying the ML criterion exist such as the reduced-search lattice decoders from which we will use the SD suggested in [40]. After applying a complex-to-real transformation of the channel in (8), the symbol dictionary C' is seen as a lattice where each emitted symbol vector \mathbf{S} is a lattice point. Due to the propagation through a noisy channel, the received vector \mathbf{Y}' is no longer a lattice point and the SD searches for the closest lattice point in a spherical region centered on \mathbf{Y}' . The choice of the radius of the sphere is crucial for the complexity reduction of the search algorithm. If the radius is judiciously chosen in function of the noise variance and the singular values of the channel, the complexity of the search algorithm becomes independent of the constellation size q and is approximated by $\mathcal{O}((MT)^6)$ [40]. This gives $\mathcal{O}(M^6)$ operations for uncoded spatial multiplexing and $\mathcal{O}(M^{12})$ for a full-rate square STBC.

III. PERFORMANCE OF CODED SYSTEMS

The benefits of using ST coding to mitigate MDL will be illustrated in a three-mode (resp. six-mode) MDM system where graded-index fibers with a parabolic index profile are installed, and have a core radius $r_c = 6 \mu\text{m}$ (resp. $r_c = 8.7 \mu\text{m}$). The field distributions of the modes are approximated by Laguerre-Gauss modes as in [14]. The simulated link is the one presented in (3) and the link parameters are the same as the ones used in Section II-A4. For the three-mode system, a gain offset of $\Delta G_{01-11} = -1.3$ dB is considered at each FMA [10]. We recall that a single polarization per mode is considered to focus solely on MDL. At the transmitter, in the uncoded scheme (or no coding: NC), a vector of 4-QAM symbols $S_{m=1:M}$ of unit energy $E_S = 1$ is sent over the modes providing a rate of 6 bits (resp. 12 bits) per time slot. In the coded case, a 3×3 (resp. 6×6) TAST code is used. At the receiver, in all scenarios, the data symbols are retrieved using a SD. The performance in terms of average bit-error-rate (BER) curves versus the symbol signal-to-noise ratio $E_S/2N_0$ per mode, of both, NC and ST-coded schemes is measured through Monte-Carlo simulations. A minimum of 100 bit errors are registered per simulation point. Three coupling scenarios with and without mode scrambling at the FMAs are presented in Fig. 3.

The first column in Fig. 3 shows the results for a three-mode MDM system. From the square marked curves corresponding to NC without mode scramblers, we notice that the SNR penalty at $\text{BER} = 10^{-3}$ induced by MDL (i.e. the gap at a given BER to a perfect MDL-free Gaussian channel) decreases from 4.2 dB for weak coupling, to 1.2 dB for medium coupling and to

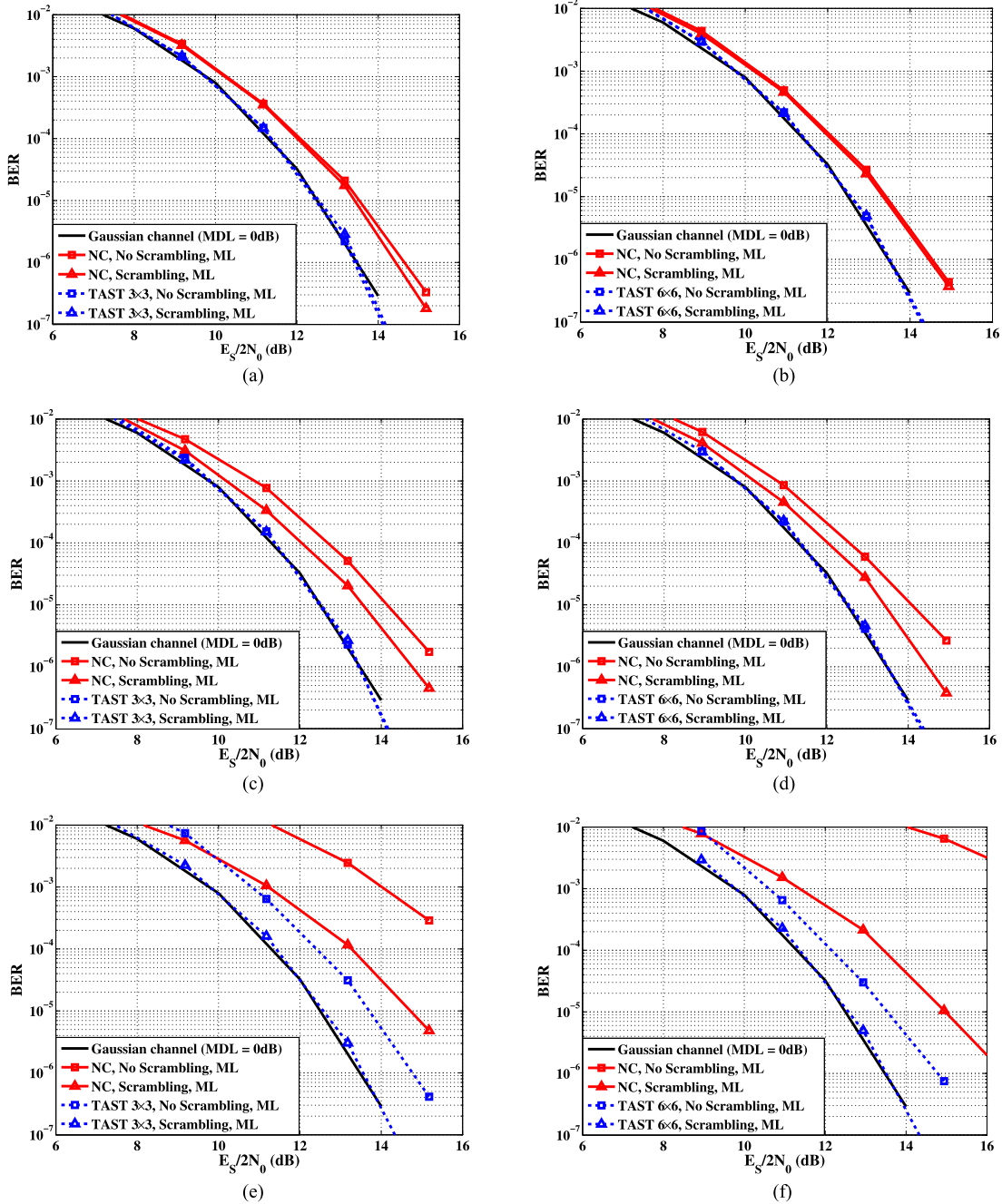


Fig. 3. Performance in terms of average BER versus SNR of 3×3 (a,c,e) and 6×6 (b,d,f) MDM systems obtained through Monte Carlo simulations (eight spans of graded-index parabolic profile fibers with a core radius $r_c = 6\mu\text{m}$ (resp. $r_c = 8.7\mu\text{m}$) and a numerical aperture $NA = 0.205$ at a wavelength $\lambda = 1550$ nm, FMAs with a maximum modal gain offset of 2 dB). (a) 3×3 system, strong coupling. (b) 6×6 system, strong coupling. (c) 3×3 system, medium coupling. (d) 6×6 system, medium coupling. (e) 3×3 system, weak coupling. (f) 6×6 system, weak coupling.

0.5 dB for strong coupling. Adding mode scramblers at FMAs (triangle marked curves), reduces these penalties to 1.5 dB for weak coupling and 0.4 dB for medium coupling while it has no effect in strong coupling regime because the modes are already fully coupled in the fiber. The same observations can be made for the six-mode MDM system (second column in Fig. 3). Again, scrambling has no effect in the strong coupling regime because the modes are fully coupled in the fiber and the MDL cannot be further reduced by the scramblers as can be seen from the MDL distributions in Fig. 2. Modal coupling and scrambling

reduce the overall MDL and thus enhance the performance of MDL-impaired MDM schemes, which was already observed in previous works [15], [17].

On the other hand, when the 3×3 TAST code is used alone (square-marked dashed curves in Fig. 3), it outperforms the scrambling solution in the scenario of weak coupling, reducing the SNR penalty at $\text{BER} = 10^{-3}$ to 1 dB for a three-mode system, which is equivalent to a coding gain of 3 dB. Furthermore, the TAST code absorbs all the MDL-induced penalty in the medium and strong coupling scenarios. Similar reductions

of penalties are observed with the 6×6 TAST code for the different coupling levels. Finally, combining the ST code with mode scrambling results in no penalty in all three-mode and six-mode schemes, and not only at a BER of 10^{-3} but for any given BER. These results prove the efficiency of ST coding solutions in mitigating MDL by averaging the losses experienced by the mode multiplexed data symbols, making it an interesting DSP solution for MDM systems. From the obtained results, we conclude that ST codes can be used as an alternative to mode scrambling or as a complementary solution to limit the number of mode scramblers in the optical link depending on the maximum gain offset of the FMAs and the coupling strength in the installed FMFs.

In [20], we showed that the performance enhancement offered by ST codes in PDL-impaired systems obeyed different criteria than those in wireless systems. An analytic expression of the minimum distance between the symbols, after propagation in PDL-impaired systems, is given in [20]; and ST-coded schemes exhibited a larger minimum distance compared to NC schemes which explains the enhanced performance. We believe that the same behavior is observed in MDL-impaired systems and leave the theoretical investigation of the observed coding gains for future studies. In the next section, we focus on the complexity and scalability of ST coding solutions.

IV. COMPLEXITY AND SCALABILITY ANALYSIS

A major advantage of ST coding is the existence of full-rate codes for larger MIMO systems where $M > 6$ modes, thus this solution can be applied to larger MDM systems such as ten-mode or Pol-Mux MDM systems. However, the downside is their decoding complexity that increases fast with the size of the MIMO system: exponentially with an exhaustive search ML decoder (q^{M^2} for a square ST code using q-QAM symbols) and in polynomial time for a SD (M^{12} for a square ST code [40]). This increased complexity can turn ST codes into a prohibitive MIMO solution for large MDM systems. Therefore, we suggest two possible variants of ST coding solutions that trade a portion of the optimal coding gains observed in the previous section for a reduction in complexity and a better scalability. The first strategy consist in replacing the optimal ML decoder with a sub-optimal low-complexity ZF-DFE, and the second one suggests replacing the square $M \times M$ code with a multi-block coding over less time slots $T < M$ in order to reduce the complexity of the ML SD by shortening the dimension of the codeword dictionary. Hence, less symbols need to be decoded at once.

A. Low-Complexity ZF-DFE Decoding

In wireless Rayleigh MIMO channels, ZF-DFE demonstrates a performance gain over the classic ZF decoder that performs a simple channel inversion, notably through its successive interference cancellation while retrieving the data symbols [41]. Decoding is performed as follows:

- 1) Given the equivalent channel model in (8), perform a QR decomposition of $\mathbf{H}_{\text{eq}} = \mathbf{Q}\mathbf{R}$ that rewrites the channel matrix as the product of \mathbf{Q} , a unitary matrix and \mathbf{R} , an upper triangular matrix.

TABLE I
COMPARISON OF PER-SYMBOL DECODING COMPLEXITIES USING DIFFERENT DECODERS OF THE EQUIVALENT $N \times N$ MIMO CHANNEL

	ZF	ZF-DFE	ML exh. search	ML sphere dec.
$N \times N$ MIMO	$\frac{N^3 + 3N^2 - N}{N}$	$\frac{N^3 + 3.5N^2 + 0.5N}{N}$	$q^N (N^2 + N)$	$\approx \frac{N^6}{N}$
Six-mode NC ($N = 6$)	53	58	28 672	7776
TAST 6×6 ($N = 36$)	1403	1423	1.7×10^{23}	6×10^7

- 2) Compute the equivalent system:

$$\tilde{\mathbf{Y}} = \mathbf{Q}^\dagger \mathbf{Y}' = \mathbf{R}\mathbf{S} + \mathbf{Q}^\dagger \mathbf{N}' \quad (10)$$

where the new noise $\mathbf{Q}^\dagger \mathbf{N}'$ remains white Gaussian given that \mathbf{Q} is a unitary matrix.

- 3) Estimate each symbol in the vector $\hat{\mathbf{S}}_{\text{ZF-DFE}}$ by solving the linear system $\tilde{\mathbf{Y}} = \mathbf{R}\mathbf{S}$. The matrix \mathbf{R} being upper triangular, the system can be solved in an iterative fashion starting from the last symbol and performing a threshold decision on each estimated symbol before feeding it to the previous equation. This translates into:

$$s_{i,i:N-1} = \frac{y_i - \sum_{j=0}^{i-1} r_{i,N-j} \hat{s}_{N-j}}{r_{i,i}}$$

$$\hat{s}_{i,i:N-1} = \lfloor s_i \rfloor \quad (11)$$

where $N = MT$ is the dimension of the system and $\lfloor \cdot \rfloor$ is the threshold decision.

The complexity of the ZF-DFE algorithm is fixed by the QR decomposition of the channel matrix and the resolution of the linear system. We computed a rough estimation of this complexity in flops that we define as the number of required complex scalar multiplications in order to decode a transmitted symbol \mathbf{S} , and compared it to the number of flops required by a ZF decoder (matrix inversion using a standard Gaussian elimination) as well as an exhaustive search ML decoder. The analytic expression of the number of flops required for decoding one q-QAM symbol in the equivalent $N \times N$ MIMO system \mathbf{H}_{eq} is given in Table I for the different decoders. Only an approximate number of operations, $\mathcal{O}(N^6)$ [40], is given for the SD whereas the exact number depends on the choice of the initial radius and the noise variance. A numerical application for an uncoded and TAST-coded 6-mode MDM system using 4-QAM symbols is also shown in Table I. It is worthy to note that the number of flops 6×10^7 for the SD 6×6 TAST scheme is still high. Obtaining the BER curve for the ML-decoded 6×6 TAST in the weak coupling case required a month-long processing on a personal PC, however we had to evaluate the optimal ML performance of the ST schemes to use them as a reference when comparing to the performance of sub-optimal schemes.

We ran Monte-Carlo simulations to obtain the performance of the ZF-DFE decoder with the previously defined 6×6 MDM system. The average BER curves of both, NC and TAST-coded schemes for three fiber coupling strengths are given in Fig 4. In all scenarios, mode scramblers are used at FMAs. First, it is

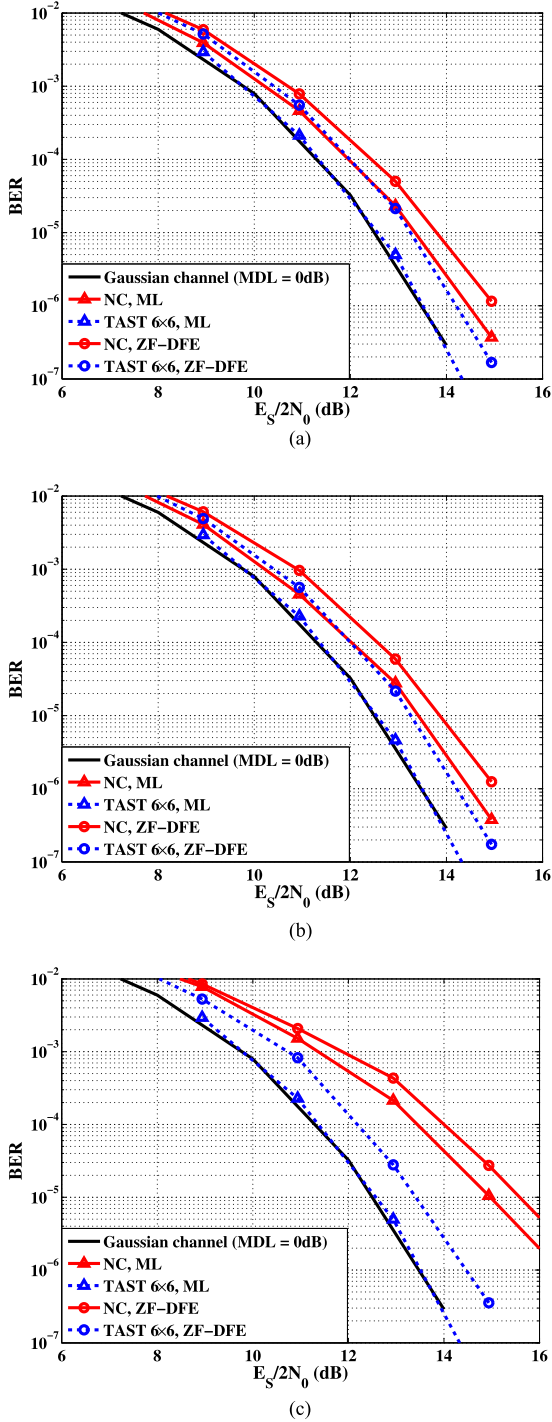


Fig. 4. Performance in terms of average BER versus SNR of ZF-DFE 6×6 ST schemes with mode scrambling, obtained through Monte Carlo simulations. (a) strong coupling. (b) medium coupling. (c) weak coupling.

obvious that the ZF-DFE decoder performs worse than the ML decoder for the NC scheme (circle marked curves) because of the noise enhancement while solving the system in (10). When ST coding is used along with ZF-DFE (dashed curves), a performance gain is obtained in all cases. At $\text{BER} = 10^{-3}$, the ZF-DFE decoded ST scheme has the same penalty of 0.4 dB as the optimal ML-decoded NC scheme for medium and strong coupling while it outperforms the NC scheme for weak coupling,

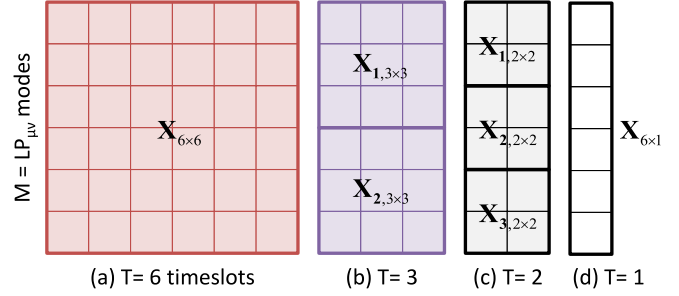


Fig. 5. Representation of codewords over modes (space) and time for the four schemes: (a) single-block 6×6 code, (b) two blocks of 3×3 codes, (c) three blocks of 2×2 codes, (d) uncoded spatial multiplexing.

providing a coding gain of 1.2 dB. Hence, with TAST coding and ZF-DFE decoding, we are reaching or outperforming the ML decoding of the NC scheme while providing a fivefold reduction in decoding complexity ($7776/1423 = 5.5$ from Table I). Moreover, the complexity of the ZF-DFE ST scheme is also independent of the constellation size of the original symbols.

Surprisingly, this performance of ST codes is completely different from the one obtained on a wireless channel where ZF-DFE decoding of the codewords would bring absolutely no gain. This is due to the need for a diversity gain in wireless communications that cannot be brought by the ZF-DFE for symmetric $N \times N$ MIMO systems. However, for the optical channel, we remark from the simulated BER curves in Fig. 3 that all curves have the same slope showing an infinite diversity order which corresponds to the behavior of a pure AWGN channel. Hence, diversity is not an issue and coding gains can be brought using sub-optimal ZF-DFE. In all investigated coupling scenarios, the low complexity decoded ST scheme for a 6×6 MDM system with experienced MDL levels as high as 10 dB is at worst at 1 dB from its corresponding optimally decoded scheme that matches the performance over an MDL-free Gaussian channel.

B. Multi-Block ST Coding

The second strategy consists in a multi-block approach. Again, we consider the previous six-mode MDM system, to study two new ML-decoded full-rate ST configurations. We suggest to limit the dimension of the ST coded system by shortening the length of the coding schemes. Lower complexity full-rate schemes over $T < 6$ time slots such as two $\mathbf{X}_{3 \times 3}$ coded blocks over $T = 3$ slots in Fig. 5(b) or three $\mathbf{X}_{2 \times 2}$ coded blocks over $T = 2$ slots in Fig. 5(c) can be considered. An important reduction of complexity is thus obtained compared to the single-block 6×6 coded scheme. Indeed, the latter requires decoding codewords of 36 data symbols at the receiver whereas the new schemes contain 18 and 12 data symbols respectively.

To illustrate the benefits of this solution, we define a two-blocks scheme where each block is coded with the 3×3 TAST code in (4) and a three-blocks scheme using the 2×2 Silver code that can be found in [20]. The strategy for allocating modes to blocks will depend on the modal gain offsets of the FMAs deployed in the optical link. The weakest modes will be coded with a privileged mode in order to average the gain

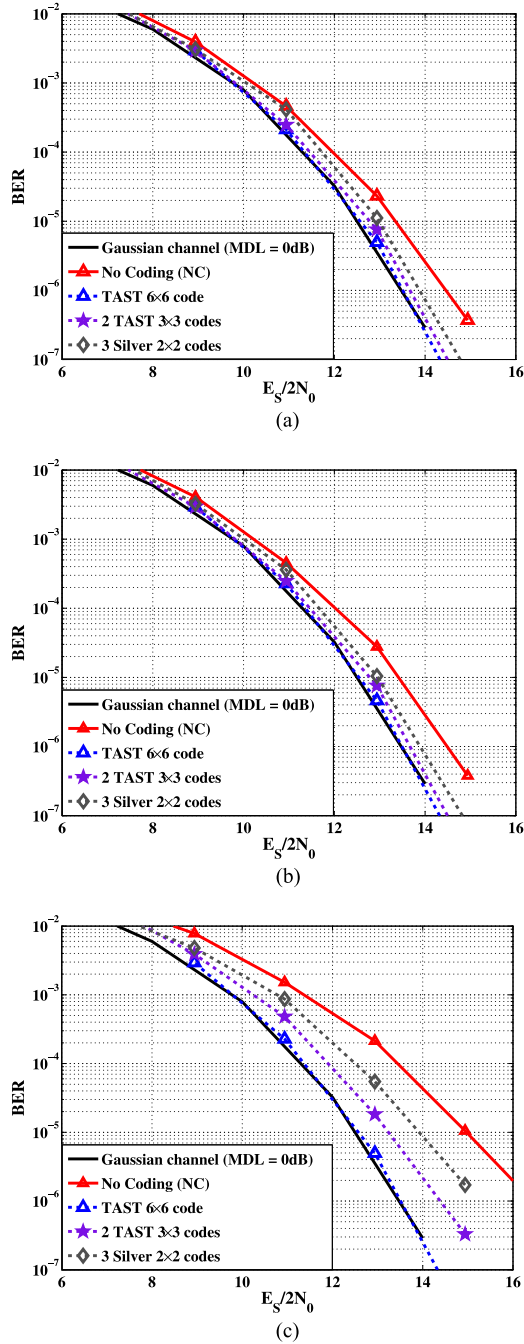


Fig. 6. Performance in terms of average BER versus SNR of multi-block ST schemes for 6×6 MDM systems with mode scrambling, obtained through Monte Carlo simulations. (a) strong coupling. (b) medium coupling. (c) weak coupling.

disparities. Hence, for the considered FMA technology, the two-blocks scheme will consist of the LP_{01} and $LP_{21a,b}$ modes in a block, and the LP_{02} with $LP_{11a,b}$ modes in another, whereas the three-blocks scheme will consist of: $\{LP_{01}, LP_{21a}\}$, $\{LP_{02}, LP_{21b}\}$ and $\{LP_{11a}, LP_{11b}\}$. For this multi-block coding solution, the vectorized channel model is the same as the single-block solution in (8) with a rearranged equivalent channel matrix \mathbf{H}_{eq} of smaller dimensions. The generator matrix \mathbf{M}_G depicting the multi-block ST-coded configuration

will consist of a block diagonal matrix with the generator matrices of the 3×3 TAST code or 2×2 Silver code on its diagonal, as illustrated here:

$$\mathbf{M}_{G,2\text{-blocks}} = \begin{bmatrix} \mathbf{M}_{G,\text{TAST}} & \mathbf{0} \\ \mathbf{0} & \mathbf{M}_{G,\text{TAST}} \end{bmatrix} \quad (12)$$

$$\mathbf{M}_{G,3\text{-blocks}} = \begin{bmatrix} \mathbf{M}_{G,\text{Silver}} & \mathbf{0} & \mathbf{0} \\ \mathbf{0} & \mathbf{M}_{G,\text{Silver}} & \mathbf{0} \\ \mathbf{0} & \mathbf{0} & \mathbf{M}_{G,\text{Silver}} \end{bmatrix} \quad (13)$$

Using Monte-Carlo simulations, we evaluate the average BER performance of the ML-decoded multi-block ST schemes over the same previously defined 6×6 MDM system. Fig. 6 shows the BER curves for three different fiber coupling strengths along with mode scramblers after each FMA. The two-blocks scheme absorbs all the SNR penalty at $\text{BER} = 10^{-3}$ for medium and strong coupling while the penalty is reduced to 0.5 dB for weak coupling. The three-blocks scheme shows an SNR penalty of 0.2 dB in medium to strong coupling scenarios and a 1 dB penalty with weak coupling. The increased penalty of the multi-block schemes is due to the fact that the codes average gains inside each block, mitigating intra-block MDL and neglecting inter-block MDL, while the fully coded scheme averages the gains over all the modes. However, the ML decoding complexity is considerably reduced. Besides, multi-block ST coding offers scalable solutions that can be extended to larger MDM systems. It can also be adapted to suit other MDM optical links where a different FMA technology is used or other MDL sources exist.

V. CONCLUSION

In this paper, we have shown, through numerical simulations, that ST coding is a promising technique for MDL-impaired MDM OFDM systems. It can be used as a standalone solution or to complement other optical components-based solutions such as mode scrambling, depending on the coupling strength in the installed fibers. The optimal ML-performance of the applied codes was investigated over three- and six-mode MDM channels with in-line MDL arising from optical amplifiers, showing a complete mitigation of MDL levels up to 10 dB. Furthermore, two strategies were presented in order to reduce the decoding complexity: on the one hand, a low-complexity decoder was shown to be near-optimal and on the other hand, a multi-block coding approach showed interesting coding gains and a large potential for scalability. The obtained coding gains can relax MDL requirements of inline components or equivalently increase the transmission reach of an MDM system. These observations pave the way for further interesting studies of ST coding solutions in SDM systems such as the application of other families of ST codes, as well as the extension beyond six modes (MDM systems with a higher number of modes M or polarization-multiplexed MDM channels where PDL can be added as another performance-limiting effect). In the future, a theoretical analysis of the observed coding gains and an MDM transmission experiment are envisaged. The following effects will be taken into account: the interaction of modal dispersion

and MDL that will result in a frequency dependent MDL, the non-whiteness of noise for a finite number of noise sources and low modal coupling levels, polarization dependent effects, and eventually the non-linear effects for high input power levels.

REFERENCES

- [1] D. Richardson, J. Fini, and L. Nelson, "Space-division multiplexing in optical fibres," *Nature Photon.*, vol. 7, no. 5, pp. 354–362, 2013.
- [2] P. J. Winzer and G. J. Foschini, "MIMO capacities and outage probabilities in spatially multiplexed optical transport systems," *Opt. Exp.*, vol. 19, no. 17, pp. 16680–16696, Aug. 2011.
- [3] S. Randel, R. Ryf, A. Gnauck, M. Mestre, C. Schmidt, R. Essiambre, P. Winzer, R. Delbue, P. Pupalais, A. Sureka, Y. Sun, X. Jiang, and R. Lingle, "Mode-multiplexed 6×20-gbd QPSK transmission over 1200-km DGD-compensated FMF," presented at the Optical Fiber Communication Conf. Exhibition/Nat. Fiber Optics Eng. Conf., Los Angeles, CA, USA, 2012, Paper PDP5C.5.
- [4] A. H. Gnauck, S. Chandrasekhar, X. Liu, S. Randel, S. Corteselli, T. Taunay, B. Zhu, and M. Fishteyn, "WDM transmission of 603-gb/s superchannels over 845km of 7-core fiber with 42.2 b/s/hz spectral efficiency," presented at the Eur. Conf. Optical Communication, Amsterdam, The Netherlands, 2012, Paper Th.2.C.2.
- [5] P. Sillard, M. Astruc, D. Boivin, H. Maerten, and L. Provost, "Few-mode fiber for uncoupled mode-division multiplexing transmissions," presented at the Eur. Conf. Optical Communication, Geneva, Switzerland, 2011, Paper Tu.5.LeCervin.7.
- [6] K. Takenaga, Y. Sasaki, N. Guan, S. Matsuo, M. Kasahara, K. Saitoh, and M. Koshiba, "Large effective-area few-mode multicore fiber," *IEEE Photon. Technol. Lett.*, vol. 24, no. 21, pp. 1941–1944, Nov. 2012.
- [7] L. Grüner-Nielsen, Y. Sun, J. W. Nicholson, D. Jakobsen, K. G. Jespersen, J. Robert Lingle, and B. Pálsdóttir, "Few mode transmission fiber with low DGD, low mode coupling, and low loss," *J. Lightw. Technol.*, vol. 30, no. 23, pp. 3693–3698, Dec. 2012.
- [8] R. Ryf, N. Fontaine, and R. Essiambre, "Spot-based mode coupler for mode-multiplexed transmission in few-mode fiber," in *Proc. IEEE Photon. Soc. Summer Topical Meeting*, Jul. 2012, pp. 199–200.
- [9] P. M. Krummrich, "Optical amplification and optical filter based signal processing for cost and energy efficient spatial multiplexing," *Opt. Exp.*, vol. 19, no. 17, pp. 16636–16652, Aug. 2011.
- [10] G. LeCocq, Y. Quiquempois, A. LeRouge, G. Bouwmans, H. ElHamzaoui, K. Delplace, M. Bouazaoui, and L. Bigot, "Few mode Er³⁺ doped fiber with micro-structured core for mode division multiplexing in the C-band," *Opt. Exp.*, vol. 21, no. 25, pp. 31646–31659, Dec. 2013.
- [11] R. Ryf, N. Fontaine, J. Dunayevsky, D. Sinefeld, M. Blau, M. Montoliu, S. Randel, L. Chang, B. Ercan, M. Esmaelpour, S. Chandrasekhar, A. Gnauck, S. Leon-Saval, J. Bland-Hawthorn, J. Salazar-Gil, Y. Sun, L. Gruner-Nielsen, R. Lingle, and D. Marom, "Wavelength-selective switch for few-mode fiber transmission," presented at the Eur. Conf. Optical Communication, London, U.K., 2013, Paper PDP1.C.4.
- [12] S. J. Savory, "Digital filters for coherent optical receivers," *Opt. Exp.*, vol. 16, no. 2, pp. 804–817, Jan. 2008.
- [13] W. Shieh, X. Yi, Y. Ma, and Y. Tang, "Theoretical and experimental study on PMD-supported transmission using polarization diversity in coherent optical OFDM systems," *Opt. Exp.*, vol. 15, no. 16, pp. 9936–9947, Aug. 2007.
- [14] S. Warm and K. Petermann, "Splice loss requirements in multi-mode fiber mode-division-multiplex transmission links," *Opt. Exp.*, vol. 21, no. 1, pp. 519–532, Jan. 2013.
- [15] A. Lobato, F. Ferreira, B. Inan, S. Adhikari, M. Kuschnerov, A. Napoli, B. Spinnler, and B. Lankl, "Maximum-likelihood detection in few-mode fiber transmission with mode-dependent loss," *IEEE Photon. Technol. Lett.*, vol. 25, no. 12, pp. 1095–1098, Jun. 2013.
- [16] K.-P. Ho and J. M. Kahn, "Mode-dependent loss and gain: Statistics and effect on mode-division multiplexing," *Opt. Exp.*, vol. 19, no. 17, pp. 16612–16635, Aug. 2011.
- [17] A. Lobato, F. Ferreira, J. Rabe, M. Kuschnerov, B. Spinnler, and B. Lankl, "Mode scramblers and reduced-search maximum-likelihood detection for mode-dependent-loss-impaired transmission," in *Proc. 39th Eur. Conf. Opt. Commun.*, London, U.K., Sep. 2013, pp. 1–3.
- [18] A. Lobato, J. Rabe, F. Ferreira, M. Kuschnerov, B. Spinnler, and B. Lankl, "Near-ML detection for MDL-impaired few-mode fiber transmission," *Opt. Exp.*, vol. 23, no. 8, pp. 9589–9601, Apr. 2015.
- [19] E. Viterbo and J. Boutros, "A universal lattice code decoder for fading channels," *IEEE Trans. Inf. Theory*, vol. 45, no. 5, pp. 1639–1642, Jul. 1999.
- [20] E. Awwad, Y. Jaouën, and G. R.-B. Othman, "Polarization-time coding for PDL mitigation in long-haul polmux OFDM systems," *Opt. Exp.*, vol. 21, no. 19, pp. 22773–22790, Sep. 2013.
- [21] E. Awwad, G. R.-B. Othman, Y. Jaouën, and Y. Frignac, "Space-time codes for mode-multiplexed optical fiber transmission systems," presented at the Adv. Photon. Commun. San Diego, CA, USA, 2014, Paper SM2D.4.
- [22] C. Okonkwo, R. van Uden, H. Chen, H. de Waardt, and T. Koonen, "Advanced coding techniques for few mode transmission systems," *Opt. Exp.*, vol. 23, no. 2, pp. 1411–1420, Jan. 2015.
- [23] A. Juarez, E. Krune, S. Bunge, and K. Petermann, "Modeling of mode coupling in multimode fibers with respect to bandwidth and loss," *IEEE J. Lightw. Technol.*, vol. 32, no. 8, pp. 1549–1558, Apr. 2014.
- [24] R. Ryf, S. Randel, A. Gnauck, C. Bolle, A. Sierra, S. Mumtaz, M. Esmaelpour, E. Burrows, R. Essiambre, P. Winzer, D. Peckham, A. McCurdy, and R. Lingle, "Mode-division multiplexing over 96km of few-mode fiber using coherent 6×6 MIMO processing," *IEEE J. Lightw. Technol.*, vol. 30, no. 4, pp. 521–531, Feb. 2012.
- [25] B. Inan, B. Spinnler, F. Ferreira, D. van den Borne, A. Lobato, S. Adhikari, V. A. J. M. Sleiffer, M. Kuschnerov, N. Hanik, and S. L. Jansen, "DSP complexity of mode-division multiplexed receivers," *Opt. Exp.*, vol. 20, no. 10, pp. 10859–10869, May 2012.
- [26] F. Ferreira, S. Jansen, P. Monteiro, and H. Silva, "Nonlinear semi-analytical model for simulation of few-mode fiber transmission," *IEEE Photon. Technol. Lett.*, vol. 24, no. 4, pp. 240–242, Feb. 2012.
- [27] F. Yaman, E. Mateo, and T. Wang, "Impact of modal crosstalk and multipath interference on few-mode fiber transmission," in *Proc. Opt. Fiber Commun. Conf. Exhib.*, Mar. 2012, pp. 1–3.
- [28] C. Koebele, M. Salsi, L. Milord, R. Ryf, C. A. Bolle, P. Sillard, S. Bigo, and G. Charlet, "40km transmission of five mode division multiplexed data streams at 100gb/s with low MIMO-DSP complexity," presented at the Eur. Conf. Optical Communication, Geneva, Switzerland, 2011, Paper Th.13.C.3.
- [29] A. Li, A. A. Amin, X. Chen, and W. Shieh, "Transmission of 107-gb/s mode and polarization multiplexed CO-OFDM signal over a two-mode fiber," *Opt. Exp.*, vol. 19, no. 9, pp. 8808–8814, Apr. 2011.
- [30] S. Arik, D. Askarov, and J. Kahn, "Effect of mode coupling on signal processing complexity in mode-division multiplexing," *J. Lightw. Technol.*, vol. 31, no. 3, pp. 423–431, Feb. 2013.
- [31] L. Gruner-Nielsen, Y. Sun, R. Jensen, J. Nicholson, and R. Lingle, "Splicing of few mode fibers," in *Proc. Eur. Conf. Optical Commun.*, Sep. 2014, pp. 1–3.
- [32] F. Ferreira, D. Fonseca, A. Lobato, B. Inan, and H. Silva, "Reach improvement of mode division multiplexed systems using fiber splices," *IEEE Photon. Technol. Lett.*, vol. 25, no. 12, pp. 1091–1094, Jun. 2013.
- [33] A. Lobato, F. Ferreira, M. Kuschnerov, D. van den Borne, S. L. Jansen, A. Napoli, B. Spinnler, and B. Lankl, "Impact of mode coupling on the mode-dependent loss tolerance in few-mode fiber transmission," *Opt. Exp.*, vol. 20, no. 28, pp. 29776–29783, Dec. 2012.
- [34] J. Carpenter, B. Eggleton, and J. Schröder, "110×110 optical mode transfer matrix inversion," *Opt. Exp.*, vol. 22, no. 1, pp. 96–101, 2014.
- [35] N. Cvijetic, E. Ip, N. Prasad, and M.-J. Li, "Experimental frequency-domain channel matrix characterization for SDM-MIMO-OFDM systems," in *Proc. IEEE Phot. Soc. Summer Topical Meeting*, Jul. 2013, pp. 139–140.
- [36] K. Guan, P. Winzer, and M. Shtaiif, "BER performance of MDL-impaired MIMO-SDM systems with finite constellation inputs," *IEEE Photon. Technol. Lett.*, vol. 26, no. 12, pp. 1223–1226, Jun. 2014.
- [37] V. Tarokh, N. Seshadri, and A. Calderbank, "Space-time codes for high data rate wireless communication: Performance criterion and code construction," *IEEE Trans. Inf. Theory*, vol. 44, no. 2, pp. 744–765, Mar. 1998.
- [38] H. El-Gamal and M.-O. Damen, "Universal space-time coding," *IEEE Trans. Inf. Theory*, vol. 49, no. 5, pp. 1097–1119, May 2003.
- [39] A. Mejri, L. Luzzi, and G.-B. Othman, "On the diversity of the naive lattice decoder," in *Proc. Int. Workshop Syst., Signal Process. Appl.*, May 2011, pp. 379–382.
- [40] O. Damen, A. Chkeif, and J. C. Belfiore, "Lattice code decoder for space-time codes," *IEEE Commun. Lett.*, vol. 4, no. 5, pp. 161–163, May 2000.
- [41] W.-J. Choi, R. Negi, and J. Cioffi, "Combined ML and DFE decoding for the V-BLAST system," in *Proc. IEEE Int. Conf. Commun.*, 2000, vol. 3, pp. 1243–1248.

Elie Awwad was born in Beirut, Lebanon, in 1988. He received the engineering diplomas in telecommunications and computer systems from the Lebanese University, Beirut, Lebanon, and TELECOM ParisTech, Paris, France, in 2011. In January 2015, he received the Ph.D. degree from TELECOM ParisTech in communications and electronics. His research work focused on emerging coding techniques for optical fiber transmission systems. His research interests include MIMO coding schemes and decoding algorithms, coherent optical fiber communication systems, and channel modeling, estimation and equalization. Since then, he is working as a Research Engineer in Alcatel-Lucent Bell Labs in Nozay, France.

Ghaya Rekaya-Ben Othman was born in Tunis, Tunisia, in 1977. She received the degree in electrical engineering from ENIT, Tunis, Tunisia, in 2000, and the Ph.D. degree from the Ecole Nationale Supérieure des Télécommunications (ENST) Paris, France, in 2004. In 2005, she joined the Department of Communication and Electronics, TELECOM ParisTech (ex-ENST) as an Assistant Professor. Since 2012, she has been a Full Professor at TELECOM ParisTech. She received the City of Paris Award of the Best Woman Scientist in 2007. Her research interests include space-time coding, lattice coding and decoding, cooperative communications, optical fiber communication, and since recently distributed storage.

Yves Jaouën received the Ph.D. degree in physics from Ecole Nationale Supérieure des Télécommunications (ENST), Paris, France, in 1993, then the HDR (Research management certificate) in 2003. He had joined the Department of Communication and Electronics, ENST (now called TELECOM ParisTech) in 1982, where he is currently a Professor. He is a Lecturer in the domain of electromagnetic fields, optics and optical communication systems. His present researches include high bit-rate coherent optical communication systems including digital signal processing aspects, new characterization techniques for advanced photonic devices, high-power fiber lasers, fiber optics, and remote sensing. He is author or coauthor of more than 180 papers in journals and communications.